Deoxidation of NiTi Alloy Melts Using Metallic Barium

Susumu Miyamoto[*1], Masatoshi Watanabe, Takayuki Narushima and Yasutaka Iguchi[*2]

Department of Materials Processing, Tohoku University, Sendai 980-8579, Japan

The deoxidation behavior of NiTi alloy melts with metallic barium was investigated. Metallic barium was added to the NiTi alloy melts held in lime (CaO) crucibles at 1673 K, and the concentrations of oxygen, barium and calcium in the melts were quantitatively measured. The oxygen content in a raw NiTi alloy bar was 660 ppm, and the oxygen content in the NiTi alloy melts just before barium addition was around 1100 ppm. Oxygen was introduced into the melts by the dissolution of lime during melting.

The addition of barium lowered the oxygen content in the melts with the formation of deoxidation product, which might be barium oxide. The oxygen content was measured to be around 350 ppm 120 s after barium addition. The barium and calcium contents were less than 10 ppm and 12 ppm, respectively, indicating that the deoxidation product was removed from the melts in a very short period of time. These results suggest that barium is an effective deoxidation element for NiTi alloy melts. Furthermore, the interaction between oxygen and barium cannot be ignored in thermodynamic considerations of the deoxidation process.   [doi:10.2320/matertrans.MRA2007219]

1. Introduction

Nickel-titanium (NiTi) alloy, a stoichiometric compound of nickel and titanium, has excellent superelastic properties and shape memory effects with a recovery strain of 10%; it is commercially used in many fields such as aerospace, biomedical and automotive industries because it also exhibits superior mechanical strength, ductility and workability.[1] NiTi alloys have relatively high corrosion resistance under aqueous conditions because they contain 50 at% of titanium and a stable passivation film is formed on their surfaces.[2,3] Therefore, NiTi alloys are applied to medical and dental devices such as dental arch wires, stents, catheters and guidewires.[3,4] In order to improve their biocompatibility or wear resistance, surface modifications using oxygen ion implantation have been investigated.[5,6] In addition to these applications, sputtered NiTi alloy thin films are also receiving considerable attention as microactuator materials.[7]

NiTi alloy ingots are industrially manufactured by vacuum induction melting with a carbon crucible and carbon mold, from which impurity carbon is introduced into the melts during the melting process. Recently, electron beam melting has been examined for application to NiTi alloys.[8–11] The carbon content in NiTi alloy melts can be suppressed to a low level by employing a water-cooled copper crucible in electron beam melting. The carbon content in the NiTi alloy ingots manufactured by electron beam melting has been reported to be 70 ppm (hereafter, ppm always denotes mass ppm.) after the melting process, while the carbon content is around 600 ppm in NiTi alloy ingots manufactured using a carbon crucible.[11] The high-vacuum operation involved in electron beam melting can minimize oxygen contamination; therefore, the carbon and oxygen contents in the ingots depend only on corresponding levels in the initial raw materials.[11] However, this also means that the oxygen content in NiTi alloy melts cannot be lowered even through the electron beam melting or vacuum induction melting because of the high chemical affinity of oxygen for titanium, although oxygen is one of the most important impurities in NiTi alloys. Oxygen is known to affect the martensite transformation and mechanical properties of NiTi alloys.[12,13] Therefore, an effective deoxidation process is required in order to control the oxygen content in NiTi alloy melts during both electron beam melting and vacuum induction melting.

Lime (CaO) is one of the candidate materials considered for use as a crucible material in the vacuum induction melting of NiTi alloys. A few studies have been reported on oxygen in titanium or titanium-aluminum melts in oxide crucibles.[14–16] Tsukihashi *et al.*[15] studied the behavior of oxygen in titanium and titanium-aluminum melts in a lime crucible and examined the interaction between calcium and oxygen. However, the behavior of oxygen in NiTi alloy melts in oxide crucibles has not been reported thus far.

The present authors thermodynamically studied the behavior of oxygen in several liquid metals,[17–20] and one of the present authors reported the deoxidation equilibrium of liquid iron in a lime crucible with barium and also reported the strong affinity of barium for oxygen in liquid iron.[17] In this study, the deoxidation behavior of NiTi alloy melts in a lime crucible using metallic barium was investigated, and the effect of barium addition on the oxygen content in NiTi alloy melts was examined.

2. Experimental

A NiTi alloy bar (ϕ: 10 mm, NEC Tokin, Sendai) was used as the raw material, which was melted in a carbon crucible using a vacuum induction process. The chemical composition of the NiTi alloy bar is shown in Table 1. The alloy of 20 g was cut from the bar, and then the surface oxide film was removed and the surface was ultrasonically cleaned in acetone before the melting experiments. The alloy was

---

[*1]Undergraduate Student, Tohoku University. Present Address: Sankyo Materials Inc., Tokyo 151-8403, Japan

[*2]Present address: Hachinohe National College of Technology, Hachinohe 039-1192, Japan

Table 1   Chemical composition of used NiTi alloy (mass%).

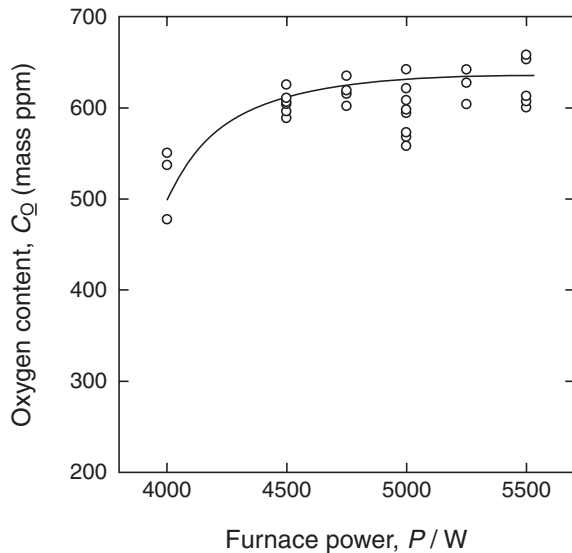| Ni	Ti	O	C
55.6	44.4	0.066	0.0344

Fig. 1 Effect of furnace power during oxygen extraction on analyzed values of oxygen content in NiTi alloy melts.
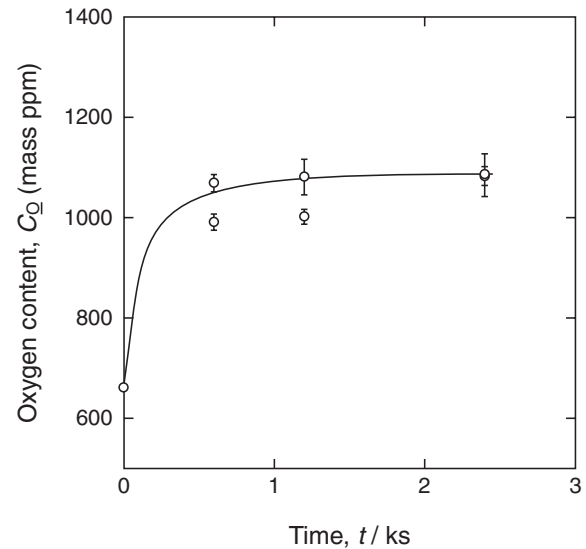

Fig. 2 Relationship between holding time and oxygen content of NiTi alloy melts in a lime crucible at 1673 K.

melted in the lime crucibles (YCH-22(S), Yoshizawa Lime Industry Co., Tokyo) of size $35^{OD} \times 26^{ID} \times 52^{H}$ mm, which were heat-treated in an argon atmosphere at 1573 K for 86.4 ks before the melting process.

NiTi alloy was set in a lime crucible, and the crucible with the alloy was placed in a vacuum induction furnace. The alloy was heated up to 1673 K under an argon gas flow of 3.3×10^{-6} m$^3 \cdot$s^{-1}. The temperature of the melt was measured using a two-color pyrometer, which was calibrated using the melting point of the NiTi alloy. After melting at 1673 K for 1.2 ks, 0.3 g of metallic barium with a purity of greater than 98% (Wako Chemical Co., Osaka) was dropped from the top of the furnace into the NiTi alloy melt. Since the handling of metallic barium was not simple, it was inserted into a nickel capsule (LECO, MI), of which mass was around 0.4 g. The nickel capsule with metallic barium was placed at the top of the furnace before each melting experiment and was dropped into the NiTi alloy melt in the lime crucible. After dropping the capsule with barium, the melt was cooled in the furnace. The maximum holding time after barium addition was 300 s.

The oxygen content in the cooled specimens was measured by the inert gas fusion-IR absorption method (TC 436E, LECO, MI). The cooled specimens were cut into pieces weighing 0.2 g each for oxygen analysis, followed by surface polishing with SiC emery paper and ultrasonic cleaning in acetone. A metal bath of carbon-saturated nickel (1.2–1.4 g per 0.2 g specimen) was used to prevent the gettering effect during the oxygen analysis.[18] Using this metal bath, the analytical values of the oxygen content in the NiTi alloy specimens became constant at furnace power levels above 4500 W, as shown in Fig. 1, and the extraction of oxygen was completed within 30 s. Consequently, the furnace power was decided to be 5500 W during oxygen extraction. The barium, calcium, nickel and titanium contents in the cooled specimens were quantitatively measured by inductively coupled plasma-atomic emission spectroscopy (ICP-AES, SPS1200A, SII, Chiba). After the surface polishing and cleaning, the alloy of 0.5 g was cut from the cooled specimens and was dissolved in an acid solution containing HF : HNO$_3$ = 1 : 2 for the analysis by ICP-AES.

3. Results and Discussion

3.1 Oxygen content in NiTi alloy melts held in lime crucible

Before the deoxidation experiments using barium, the oxygen content in the NiTi alloy melts held in a lime crucible was measured in order to determine the initial oxygen content. Figure 2 shows the relationship between the holding time and the oxygen content of the NiTi alloy melts in a lime crucible at 1673 K. The oxygen content of a raw NiTi alloy bar was 660 ppm (see Table 1), while it increased to around 1100 ppm after melting in a lime crucible for 0.6 ks. It is considered that oxygen was introduced into the NiTi alloy melts by the dissolution reaction of lime, as shown in eq. (1)

$$CaO(s) = \underline{Ca}(\text{in NiTi melt}) + \underline{O}(\text{in NiTi melt}) \qquad (1)$$
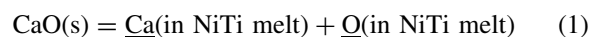
Since a constant oxygen content was obtained after holding for 0.6 ks, for the deoxidation experiments, metallic barium was dropped into the alloy melts after holding in a lime crucible at 1673 K for 1.2 ks. That is, the oxygen content in the NiTi alloy melts just before the addition of barium was around 1100 ppm.

3.2 Deoxidation of NiTi alloy melts using metallic barium

Figure 3 shows the change in the oxygen content in the NiTi alloy melts with holding time after barium addition. The oxygen content of around 1100 ppm before barium addition decreased drastically to 350 ppm. The value of 350 ppm is approximately half that in a raw NiTi alloy bar, 660 ppm. This decrease in the oxygen content was caused by the reaction of barium with the dissolved oxygen in the NiTi alloy melts, as described in eq. (2).
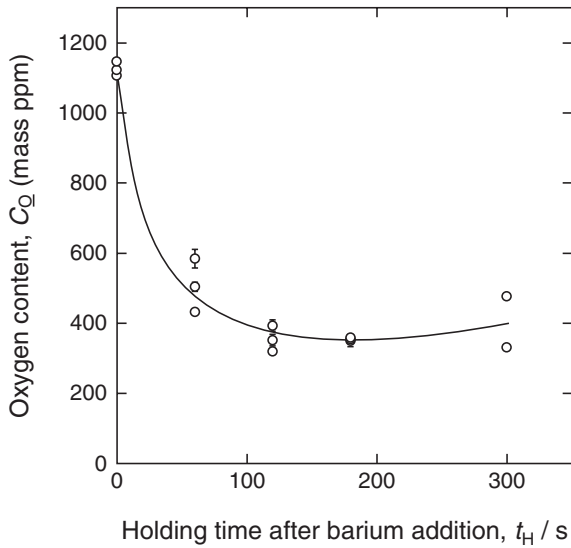
Fig. 3   Change in oxygen content in NiTi alloy melts with holding time after barium addition at 1673 K.
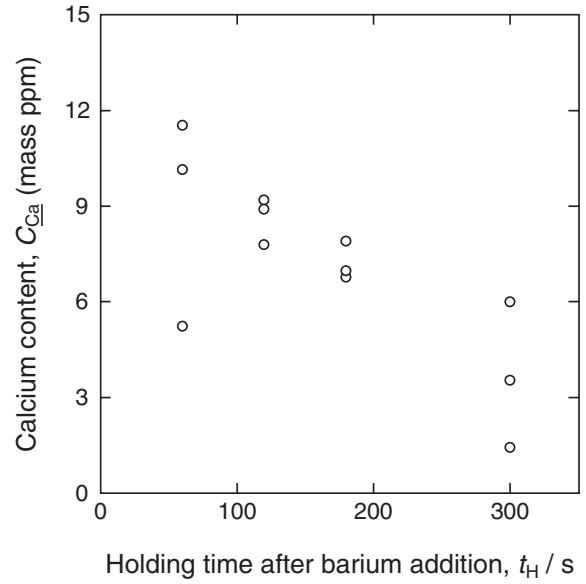

Fig. 5   Change in calcium content in NiTi alloy melts with holding time after barium addition.
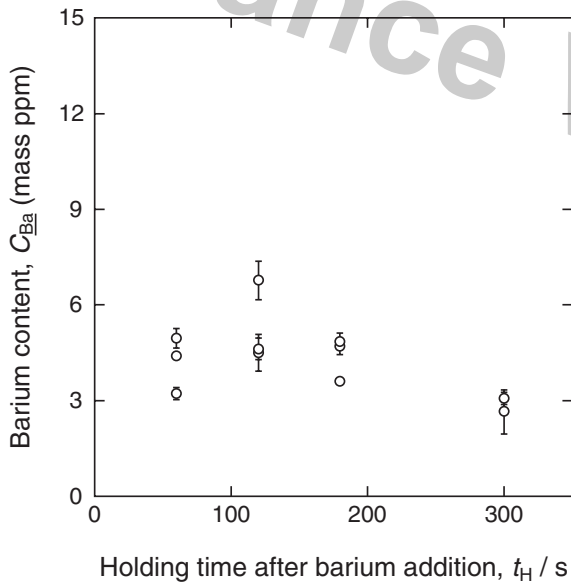

Fig. 4   Change in barium content in NiTi alloy melts with holding time after barium addition.
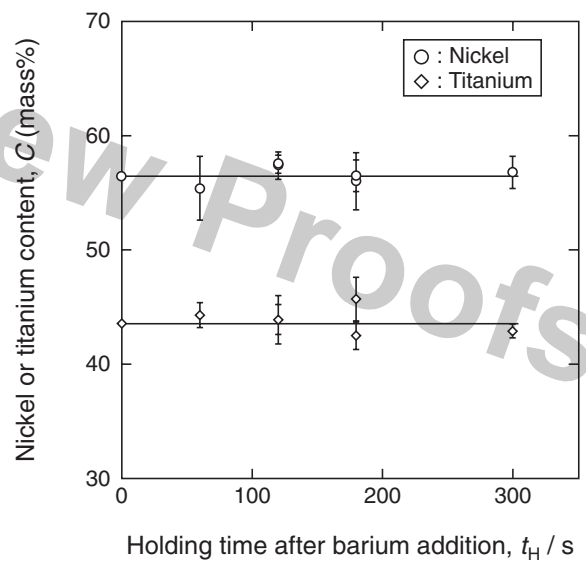

Fig. 6   Change in nickel and titanium contents in NiTi alloy melts with holding time after barium addition.

$$\underline{Ba}(\text{in NiTi melt}) + \underline{O}(\text{in NiTi melt}) = BaO(s) \qquad (2)$$

The oxidation product was considered to be barium oxide, BaO. Figure 4 shows the barium content in the NiTi alloy melts as a function of the holding time after barium addition. The barium content was less than 10 ppm. The analytical value in ICP-AES represents the total barium content in the specimen. Therefore, the results suggest that the deoxidation product, barium oxide, formed by the reaction shown in eq. (2) was removed from the melts in very short period of time, such as 60 s. The material balance calculations show that the approximately half the added barium reacted with oxygen to form barium oxide, suggesting that the other part was consumed by vaporization during the addition or melting

process. It was observed that the barium contents in the NiTi alloy melts decreased 180 s after barium addition, which might be caused by the vaporization of barium from the melts. As shown later, the oxygen contents increases with decreasing barium contents in low barium content region (see Fig. 8). Therefore, the slight increase of oxygen contents was observed 180 s after barium addition as shown in Fig. 3. Figure 5 shows the calcium content in the melts after barium addition; it was less than 12 ppm.

The changes in the nickel and titanium contents in the melts after barium addition are shown in Fig. 6. The initial nickel and titanium contents before barium addition shown in Fig. 6 were the calculated values including the mass of the nickel capsule used for the addition of barium. No significant
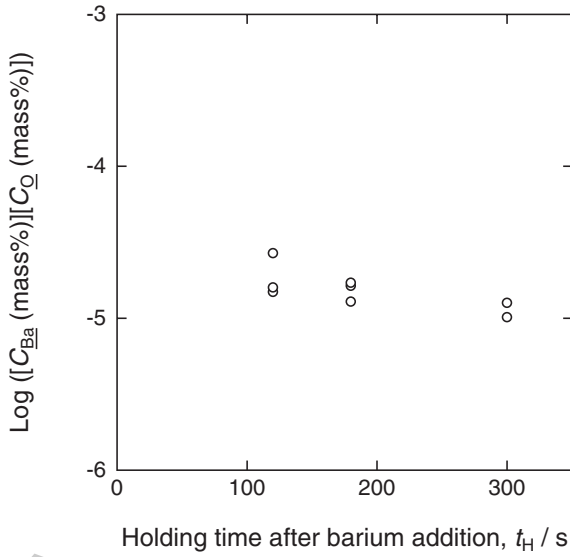
Fig. 7 Change in log([$C_{\underline{Ba}}$(mass%)][$C_{\underline{O}}$(mass%)]) with holding time after barium addition.
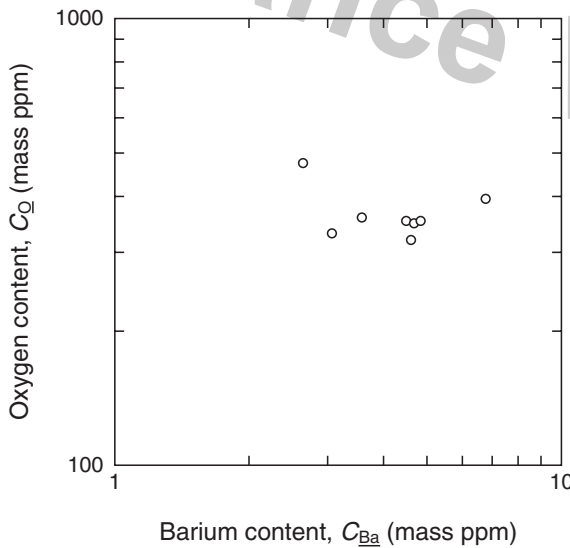

Fig. 8 Relationship between barium and oxygen contents in NiTi alloy melts.

change was observed in the nickel and titanium contents with the holding time and it was confirmed that the vaporization of nickel or titanium from the melts was not remarkable during the melting of the NiTi alloy in the lime crucibles at 1673 K.

The equilibrium constant of eq. (2), K_2, can be expressed as in eq. (3).

$$K_2 = \frac{a_{BaO}}{a_{\underline{Ba}}a_{\underline{O}}} \tag{3}$$

where $a_{\underline{Ba}}$ and $a_{\underline{O}}$ are the activities of barium and oxygen in the NiTi alloy melts, respectively, and the standard state for the activities are taken as 1 mass% in the NiTi alloy melts. The activity of barium oxide, a_{BaO}, can be set to be unity, assuming the deoxidation product is pure barium oxide. Since $a_{\underline{i}}$ (i: Ba or O) can be expressed as $f_{\underline{i}}[C_{\underline{i}}(\text{mass}\%)]$ using the

active coefficient of i, f_i, Equation (3) can be rewritten as eq. (4).

$$
\begin{aligned}
K_2 &= \frac{1}{f_{\underline{Ba}}[C_{\underline{Ba}}(\text{mass}\%)]f_{\underline{O}}[C_{\underline{O}}(\text{mass}\%)]} \\
&= \frac{1}{f_{\underline{Ba}}f_{\underline{O}}} \cdot \frac{1}{[C_{\underline{Ba}}(\text{mass}\%)][C_{\underline{O}}(\text{mass}\%)]}
\end{aligned} \tag{4}
$$

Figure 7 shows the relationship between the holding time and the value of log[$C_{\underline{Ba}}$(mass%)][$C_{\underline{O}}$(mass%)], assuming that the equilibrium of eq. (2) was established 120 s after barium addition. The value of log[$C_{\underline{Ba}}$(mass%)][$C_{\underline{O}}$(mass%)] is around −4.9, and a decreasing trend in the value with the holding time was detected. The relationship between log[$C_{\underline{Ba}}$(mass%)] and log[$C_{\underline{O}}$(mass%)] is shown in Fig. 8, where a simple linear relationship was not observed. If both oxygen and barium obey Henry's law, that is, the activity coefficients of both oxygen and barium are equal to unity, the slope of the relationship between log[$C_{\underline{Ba}}$(mass%)] and log[$C_{\underline{O}}$(mass%)] should be −1. Therefore, the results shown in Fig. 7 and Fig. 8 suggested that the interaction between barium and oxygen could not be ignored in NiTi alloy melts. In order to evaluate the interaction, further studies on barium deoxidation with various initial oxygen contents and the amounts of added barium are required.

In this study, barium deoxidation was applied to NiTi alloy melts in a lime crucible at 1673 K for the first time. The oxygen content in the NiTi alloy melts could be lowered to 350 ppm by means of deoxidation using metallic barium, and furthermore, it was found that the barium content in the melts was less than 10 ppm after deoxidation. This barium deoxidation process can be applied to industrial vacuum induction melting for NiTi alloys in carbon crucibles and to electron beam melting. Since no increase in the oxygen content occurs in these processes before the addition of barium, barium deoxidation for NiTi alloys melts was considered to be more effective compared with that for the melts in lime crucible. In addition, barium deoxidation might also be applicable to titanium and titanium alloys melts, for which an effective deoxidation process has not yet been reported.

4. Conclusions

Barium deoxidation of NiTi alloy melts in lime crucibles at 1673 K was investigated, and the effect of barium addition on the oxygen content in the melts was examined, yielding the following results.

(1) The oxygen content in the NiTi alloy melts increased from 660 ppm, which was oxygen content in a raw NiTi alloy bar, to 1100 ppm during the melting process in a lime crucible before barium addition.

(2) The oxygen content in the NiTi alloy melts decreased to 350 ppm after barium addition. The barium content in the melts was less than 10 ppm after barium addition. These results suggest that barium is an effective element for the deoxidation of NiTi alloy melts.

(3) It was found that the interaction between barium and oxygen in the NiTi alloy melts cannot be ignored in thermodynamic considerations of the deoxidation process.

REFERENCES

1) H. Hosoda and S. Miyazaki: J. Jpn. Soc. Mech. Eng. **107** (2004) 509–515.
2) H. Hosoda and S. Miyazaki: *Basics and Applications of Metallic Biomaterials*, (ICP, 2000) pp. 133–149.
3) Y. Oshida and S. Miyazaki: Zairyo-to-Kankyo **40** (1991) 834–844.
4) P. Filip: *Titanium in Medicine*, (Springer, 2001) pp. 53–86.
5) S. Mändel, A. Fleischer, D. Manova and B. Rauschenbach: Surf. Coat. Tech. **200** (2006) 6225–6229.
6) L. Tan, R. A. Dodd and W. C. Crone: Biomaterials **24** (2003) 3931–3939.
7) S. Miyazaki and A. Ishida: Mater. Sci. Eng. A **273–275** (1999) 106–133.
8) H. Matsumoto: J. Mat. Sci. Lett. **10** (1991) 417–419.
9) H. Matsumoto: J. Mat. Sci. Lett. **10** (1991) 596–597.
10) J. Obuto, O. D. Rigo, C. M. Neto, M. J. Kaufman and P. R. Mei: J. Phys. IV Fr. **112** (2003) 873–876.
11) J. Obuto, O. D. Rigo, C. M. Neto and P. R. Mei: Mater. Sci. Eng. A **438–440** (2006) 679–682.
12) Y. Shugo, S. Hanada and T. Honma: Bull. Rea. Inst. Mineral Dressing and Metall. **41** (1985) 23–34.
13) *Shape Memory Materials*, ed. by K. Otsuka and C. M. Wayman, (Cambridge University Press, 1998) pp. 71–73.
14) F. Maeda, T. Yahara, K. Mitugi and T. Ikeda: Mater. Trans. JIM **34** (1993) 599–603.
15) F. Tsukihashi, E. Tawara and T. Hatta: Metall. Mater. Trans. B **27B** (1996) 967–972.
16) Y. Kobayashi and F. Tsukihashi: High Temp. Mater. Res. **19** (2000) 211–218.
17) S. Kato, Y. Iguchi and S. Ban-ya: Tetsu-to-Hagane **78** (1992) 253–259.
18) T. Narushima, K. Matsuzawa, Y. Mukai and Y. Iguchi: Mater. Trans. JIM **35** (1994) 522–528.
19) T. Narushima, K. Matsuzawa, M. Mamiya and Y. Iguchi: Mater. Trans. JIM. **36** (1995) 763–769.
20) K. Tajima, T. Ogasawara, T. Narushima, C. Ouchi and Y. Iguchi: Mater. Trans. **42** (2001) 2434–2439.